



Modelling and assessment of earthquake ground response in areas characterised by a thick buried low-velocity layer

Daniela Farrugia¹ · Pauline Galea¹ · Sebastiano D'Amico¹

Received: 7 April 2020 / Accepted: 2 September 2020 / Published online: 18 September 2020
© Springer Nature B.V. 2020

Abstract

It is known that local geology can alter the ground motion characteristics at a particular site. Whereas some sites are characterised by outcropping low-velocity layers, others might have buried ones of considerable thickness which might still be a cause of ground motion amplification. The Maltese islands (Central Mediterranean) provide a good case study for profiles with a buried low-velocity layer. Parts of the islands are characterised by Upper Coralline Limestone covering a soft Blue Clay layer of considerable thickness (up to 75 m). This gives rise to a velocity inversion and makes the travel-time average shear-wave velocity (V_S) in the upper 30 m not suitable for seismic microzonation purposes. This study presents a comprehensive site response analysis for such areas. Previously obtained shear-wave velocity (V_S) profiles were used as an input to the equivalent linear programme SHAKE2000. Maps of amplification factors and 5% damped elastic response spectra confirm that the clay, even when buried under a hard outcropping layer, can still produce significant amplifications at frequencies which are of engineering interest when considering the recent urbanisation patterns. Moreover, the suitability of the V_{S30} and the travel-time average shear-wave velocity till bedrock parameters as proxies for site response was investigated, with the results highlighting the inadequacy of these parameters for sites characterised by buried low-velocity layers and the necessity for site-specific response studies.

Keywords Site response · Low-velocity layer · Validity of VS30 · site classification

1 Introduction

The Maltese islands have suffered damage from earthquakes in the historical past (Galea 2007), the most serious being the event of 11 January 1693, due to a magnitude 7.4 earthquake in SE Sicily (Guidoboni et al. 2018). Other large earthquakes in southern Greece, as well as more moderate ones in the Sicily Channel, have also caused building damage. The majority of the buildings are of load-bearing unreinforced masonry, and recently the islands have seen the emergence of numerous apartment blocks of 5–7 storeys as well as a number of existing and planned tower blocks exceeding 20

✉ Daniela Farrugia
daniela.farrugia@um.edu.mt

¹ Department of Geosciences, University of Malta, Msida, Malta

storeys. The public perception about seismic risk remains generally one of negligence and complacency.

A national strategy needs to consider and integrate a number of approaches, such as probabilistic/deterministic seismic hazard assessment, evaluation of local seismic site response as a function of surface geology, and estimates of ground motion parameters (ground acceleration and ground velocity) in realistic earthquake scenarios. Such estimates can then be used to predict the behaviour of typical local constructions in response to ground shaking.

The islands composing the Maltese archipelago are characterised by a four-layer sequence of limestones and clays (Pedley et al 1978) (Fig. 1). The western half of the archipelago is characterised by Upper Coralline Limestone (UCL) plateaux and hillcaps, reaching thicknesses up to 162 m (1977), covering a Blue Clay (BC) layer which can be up to 75 m thick. This results in a seismic velocity inversion in the stratigraphy.

In recent years, studies on local seismic site response have been carried out both on a national scale, as well as in the form of microzonation studies in some areas of the archipelago. These studies, through the recording of ambient seismic noise and analysis of horizontal-to-vertical spectral ratios (H/V), have revealed that the western half of Malta, and the island of Gozo, where the clay layer is present within the lithostratigraphy, have the clear potential to amplify ground motion in specific frequency ranges, as opposed to the eastern half of the archipelago where the outcropping rock is mainly the Lower Globigerina Limestone which may be considered as bedrock (Pace et al. 2011;

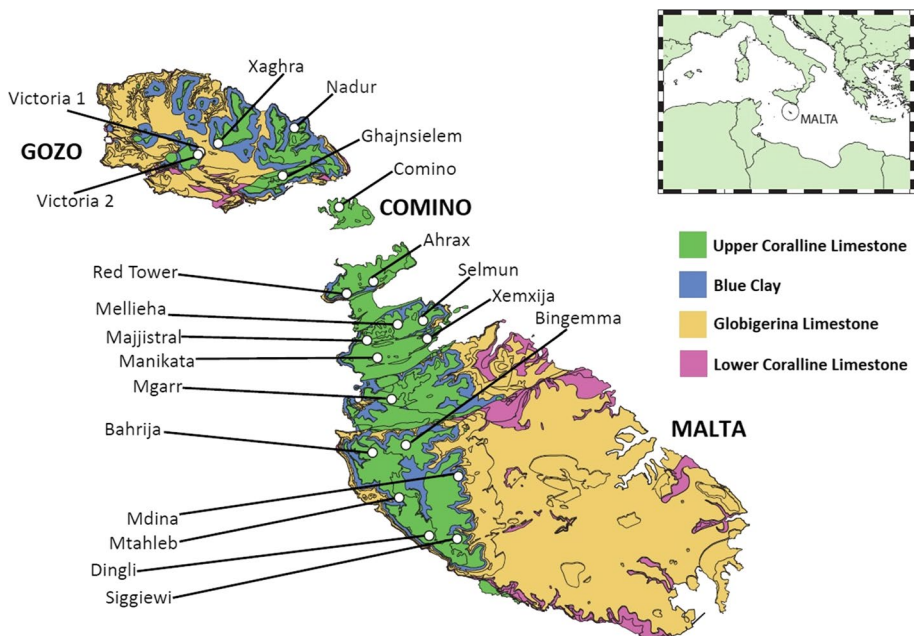


Fig. 1 a Simplified geological map of the Maltese islands with location and names of the investigated sites (Oil Exploration Directorate 1993). Inset shows the location of the Maltese islands in the Central Mediterranean

Panzer et al. 2013; Vella et al. 2013). These results have important implications on the building seismic action determination.

Various building codes, including the Eurocode 8, use the V_{S30} parameter as a proxy for site amplification because it can be easily obtained at a relatively low cost. However, using a single parameter to represent the entire V_S profile cannot quantify properly the effects of the real impedance contrast/s, which is one of the main sources of soil amplification. Moreover, the EC8 classification scheme uses very broad categories, each including a large variety of soil types and thicknesses. For example, the EC8 site category B includes very dense sand-gravels to very stiff-hard clays, having a thickness of several tens of meters and V_{S30} from 360 to 800 m/s (Pitilakis et al. 2013). Nonetheless, there is no reference to sites with thick buried low-velocity layers in the EC8 classification scheme.

Recent studies have questioned the use of V_{S30} as a proxy for site amplification (e.g. Castellaro et al. 2008; Wald and Mori 2000; Park and Hashash 2004). Castellaro et al. (2008) argue that even though the shear-wave velocity of the subsoil should have a role in the site effect assessment because it is related to soil rigidity, seismic amplification is too complex to be related to a single parameter based on the first 30 m of subsoil. As argued by Di Giacomo et al. (2005), the V_{S30} might represent a problem when velocity inversions are present in the stratigraphy whilst Ozcep et al. (2013) show the inadequacy of V_{S30} in the case of complex basin structures. Moreover, the role of sediments deeper than 30 m in seismic amplification was demonstrated by Frankel et al. (2002), and Park and Hashash (2004) demonstrated the role of deeper sediments (> 30 m) in seismic amplification. As regards the V_{S30} -based soil classification schemes (such as EC8 and NEHRP), Park and Hashash (2004) also observe that the use of NEHRP site-correction coefficients overestimates seismic ground motion at short periods and underestimates seismic ground motion at long periods for the cases of thick deposits. Wald and Mori (2000) also identified a large degree of scatter in the observed amplification within each class of the NEHRP scheme, whilst Stewart et al. (2003) found that it is not optimised for long periods ($T > 1$ s) with respect to both the dispersion and distinction criteria.

Efforts have been made to identify several alternative or supplementary indicators for site response. These include depth-to-basement (Steidl 2000), average V_S over depths other than 30 m (Gallipoli and Mucciarelli 2009) and fundamental site period/frequency (Luzi et al. 2011; Di Alessandro et al. 2012; Peruzza et al. 2017). New classification schemes based on the above-mentioned parameters are also being proposed. Luzi et al. (2011) and Di Alessandro et al. (2012) devised new classification schemes which are based on the fundamental frequency, f_0 or a combination of the V_{S30} and f_0 . Pitilakis et al. (2013) proposed a new classification which uses parameters such as the thickness of soil deposits, the average shear-wave velocity to the seismic bedrock and the fundamental period of the site.

In this study, experimentally determined V_S profiles characterised by a buried low-velocity layer were evaluated for site response using the equivalent-linear code SHAKE2000 (Ordonez 2011). Results in terms of 5% damped elastic response spectra were then used to assess the expected amplification at these sites. Moreover, to understand the implications of low-velocity layers on site class definition and hence on the correct prediction of their response to ground shaking, various tests using the resulting response spectra were conducted to investigate the following:

- The effects of the buried clay layer;
- The validity of parameters such as V_{S30} and $V_{Sbedrock}$ for site response;
- The validity of site classification of building codes, such as Eurocode 8.

2 Tectonic features and geological setting of the Maltese islands

The Maltese archipelago is made up of three islands (Malta, Gozo and Comino) and covers an area of around 316 km². The islands lie in the Sicily Channel (inset in Fig. 1) on a relatively stable plateau of the African foreland, known as the Pelagian Platform, about 200 km south of the convergent segment of the Europe-Africa plate boundary that runs through Sicily.

The Pelagian Platform separates the deep Ionian Basin from the Western Mediterranean. Its sea-bed topography is characterised mainly by a number of deep NW trending grabens, namely the Pantelleria Graben, Linosa Graben and Malta Graben, collectively termed the Pantelleria Rift or Sicily Channel Rift Zone (SCRZ). The depth of the Pantelleria Rift reaches a maximum of around 1700 m. The Hyblean Platform, between Malta and SE Sicily, is separated from the deep Ionian basin to the east by the steep Malta Escarpment (Pedley et al 2002).

The Maltese islands were formed as marine sediments during the Oligocene and Miocene epochs and were uplifted around 10 million years ago for the first time, as a result of incipient rifting in the Sicily Channel. The islands are made up of four strata of lime-rich sedimentary rocks, with the composition and texture of each layer depending amongst other things, on the grain size of the sediment and depth of deposition (Pedley et al. 2002). Starting from the bottom and oldest, the formations are as follows: the Lower Coralline Limestone (LCL), the Globigerina Limestone (GL), the Blue Clay (BC) and the Upper Coralline Limestone (UCL) (refer to Fig. 1).

The compact LCL is exposed mainly as cliff faces in the south-west coast. It is non-homogeneous and composed of five different ‘facies’ according to the depositional environment of the sediments (Pedley et al. 2002; Gatt et al. 2009; Gatt 2012). The GL covers large areas of central and southern Malta and Gozo (Magri 2006). It is a chalky and soft yellowish fine-grained limestone, which is further subdivided into three layers separated by two thin hardground conglomerate layers.

The Blue Clay layer is the softest in the layer package and is easily erodible. It is mostly found beneath the UCL which is the youngest of the layers and can have variable characteristics, ranging from fractured and friable to highly compact. As can be seen from Fig. 1, the western half of Malta and some areas in Gozo retain the full sedimentary sequence (Pedley et al. 2002).

3 Methodology

The evaluation of local seismic response was performed numerically using the equivalent-linear earthquake site response code SHAKE2000 (Ordóñez 2011). The code requires three main inputs: a shear-wave velocity profile representative of the site, an input motion acceleration time-history, and the modulus reduction and damping curves for each geological layer. In the following section, the methods for obtaining each of the three input parameters will be discussed.

3.1 Obtaining the shear-wave velocity profiles

Shear-wave velocity profiles had been previously obtained at 20 sites on the islands, shown in Fig. 1, using surface wave measurements (Farrugia et al. 2016). At each investigated site, single- and multi-station seismic ambient noise recordings were collected as explained in Farrugia et al. (2016). The single-station time-series were used to obtain the H/V curve (Nakamura 1989), which gives a peak at the fundamental resonance frequency of the site in the range of 1–2 Hz (refer to Farrugia et al. 2016). The phase-velocity dispersion curves were obtained by processing the array data using the ESAC (Extended Spatial Auto-Correlation; Ohori et al. 2002) technique. The H/V and dispersion curves for each site were then jointly inverted using a Genetic Algorithm (Yamanaka and Ishida 1996; Picozzi and Albarello 2007).

For each site, the inversion algorithm was set to run 10 times, each time starting from a random model. From the 10 best models, the model having the lowest misfit was then chosen as the representative profile of the site and was used for site response analysis. We remark that in a site-specific investigation, it would be advisable to run the analysis using more than one possible velocity profile; however, this study was intended to demonstrate the effect of the buried low-velocity layer in a nation-wide context, and therefore the model with the lowest misfit was consistently chosen at all sites. Figure 2 shows the selected V_S profiles for each site and a stratigraphic interpretation. In addition, the V_{S30} for each profile was computed and is listed in the same figure. The GL layer was chosen as the bedrock reference layer because its velocity is greater than 800 m/s (except in Manikata and Mdina). Table 1 shows the V_S ranges for the three lithotypes obtained from all the studied sites.

3.2 Obtaining the input acceleration time histories

In order to determine the site-specific frequency response at the chosen locations, it was required to select a set of input acceleration time histories that would be compatible with the national seismic hazard parameters. Based on research conducted to date, and pending the final establishment of national seismic design parameters for the Maltese islands, a plausible value for the mean value of PGA corresponding to a 475-year return period, on rock sites, is 0.08 g (Panzeria et al. 2015). Taking into consideration the seismic history as well as the seismotectonic background, this seismic hazard contains contributions both by moderate magnitude events ($M=5.0\text{--}6.0$) at short distances ($d=10\text{--}40$ km) as well as by high magnitude events ($M=6.5\text{--}8.0$) at distances larger than 90 km (Panzeria et al. 2015).

SHAKE2000 allows the use of both synthetic as well as real acceleration time histories as input motion at the base of the stratigraphic layer package. Synthetic data are known to suffer from an excessive number of cycles of strong motion and consequently possess unreasonably high energy content (Bommer and Acevedo 2004). Moreover, the available, and frequently used code, EXSIM, only simulates the high-frequency wave-field (> 1 Hz). On the other hand, no real data, recorded on the Maltese islands, corresponding to design earthquake parameters, are available. We have therefore decided to take the approach of ‘spectrum matching’, in which a suite of seven real accelerograms was selected from the European Strong Motion Database using the REXEL code (Iervolino et al. 2010), whose average spectra matched closely a chosen target spectrum (Smerzini et al. 2014). For the latter, we selected the EC8 Type 1 spectrum, anchored at a PGA of 0.08 g, given that the earthquake with the largest contribution to the seismic

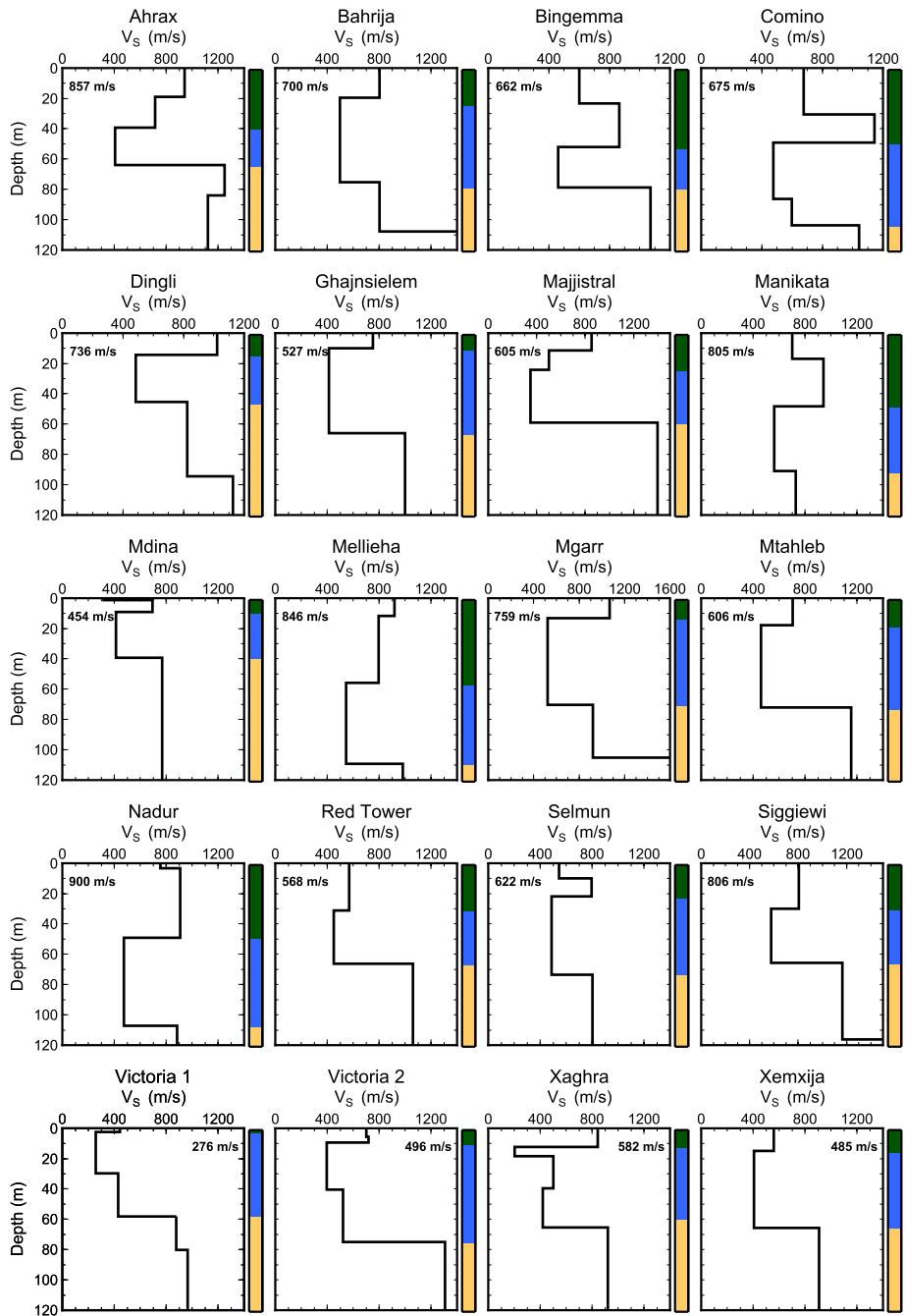


Fig. 2 The shear-wave velocity profile of each site obtained using geophysical investigations and a stratigraphic interpretation (UCL-green, BC-blue, GL-cream). The V_{S30} value for each profile is shown in the figure

Table 1 The V_s ranges for each lithotype obtained from all the studied sites

| Lithotype | V_s range (m/s) |
|-----------|-------------------|
| UCL | 550–1100 |
| BC | 350–600 |
| GL | 700–1400 |

hazard has magnitude > 5.5 (1693 M7.4 event in SE Sicily). In other words, we have considered the far-field scenario as our case study. The use of seven accelerograms, and the subsequent averaging of the response spectra, is recommended in order to cover a wider range of earthquake types or magnitude-distance combinations (Pagliaroli and Lanzo 2008).

The search was conducted for magnitudes between 6.5 and 8.0 and distances between 60 and 200 km (Panzera et al. 2015). Only earthquakes recorded at stations installed on class A sites, according to the EC8, were chosen. The selected records were scaled to the target PGA by applying a constant scaling factor. As required by the EC8, a condition was set before the search such that the average elastic spectrum would not underestimate the code spectrum by more than 10%. EC8 does not provide any value for the upper limit; however, an upper tolerance of 30% was chosen as recommended in Iervolino et al. (2010). The input acceleration time histories were applied at the top of the GL layer which is the bedrock reference layer as described in Sect. 3.2.

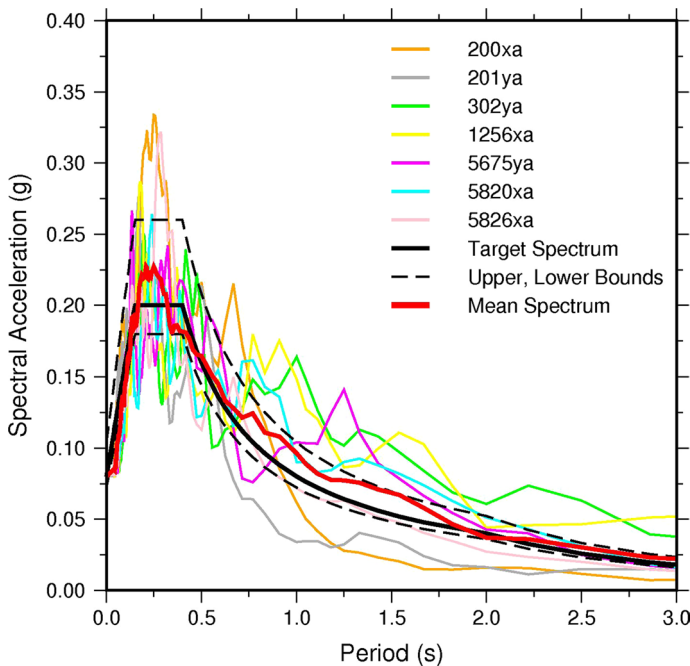


Fig. 3 The response spectra of the selected input motions (scaled time history accelerograms). Event information is given in Table 2

Table 2 The parameters of the seven selected acceleration time histories of earthquakes from the European Strong Motion Database (Luzi et al. 2016)

| Code | Earthquake name | Date | MW | Epical distance (km) | Fault mechanism | Scale factor |
|--------|-----------------|------------|-----|----------------------|-----------------|--------------|
| 200xa | Montenegro | 15/04/1979 | 6.9 | 65 | Thrust | 0.36 |
| 201ya | Montenegro | 15/04/1979 | 6.9 | 105 | Thrust | 1.07 |
| 302ya | Campano | 23/11/1990 | 6.9 | 92 | Normal | 5.08 |
| 1256xa | Izmit | 17/08/1999 | 7.6 | 92 | Strike-slip | 2.27 |
| 5675xa | Montenegro | 15/04/1979 | 6.9 | 180 | Thrust | 3.67 |
| 5820ya | Strofades | 18/11/1997 | 6.6 | 136 | Oblique | 0.87 |
| 5826xa | Strofades | 18/11/1997 | 6.6 | 90 | Oblique | 1.21 |

Plots of the scaled spectra of the chosen earthquakes together with the EC8 target spectra are presented in Fig. 3. Table 2 displays the information about the chosen suite of records.

3.3 Choosing the modulus reduction and damping curves

The modulus reduction and damping curves were chosen from the curves available in SHAKE2000 which reasonably represent the stratigraphical geotechnical properties available at various sites on the islands (A Mifsud 2019, personal communication). These are shown in Fig. 4. Conducted sensitivity studies (e.g. Barani et al. 2013) have shown that these have minimal effect on the obtained results.

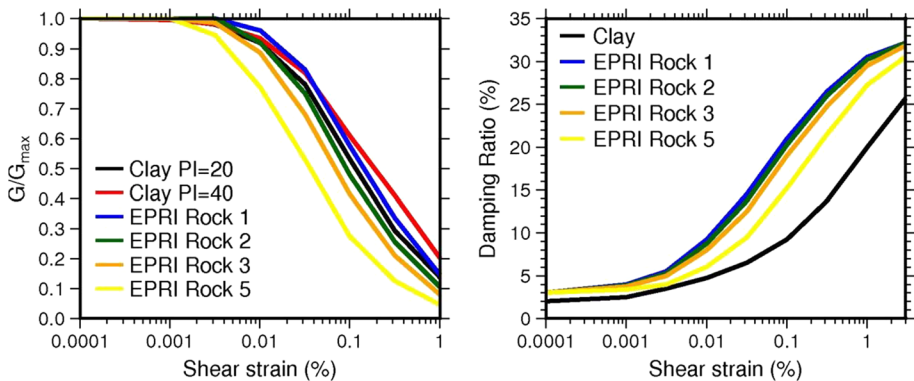


Fig. 4 The modulus reduction and damping curves used in this study. The EPRI curves were used to model the limestone layer according to their depth (the deepest being EPRI Rock 5) whilst the clay curves were used to model the clay layers

4 Results and discussion

The SHAKE2000 software provides PGA values, the theoretical transfer function and the response spectra as output results, amongst others.

4.1 The response spectra

In Fig. 5, the 5% damped elastic response spectra obtained for each site are shown. The spectra are grouped according to the corresponding EC8 site class, based on the computed V_{S30} as displayed in Fig. 2. Five sites, with a V_{S30} result larger than 800 m/s, have been classified as EC8 Site Class A. The response spectra for three of these sites lie below the EC8 target spectrum at the plateau range of frequencies; however, at two sites (Ahrax and Siggiewi), the spectrum shows a well-defined peak which is up to 50% higher than the target spectrum and more consistent with a Class B spectrum. It is also considerably shifted towards longer periods. Indeed, all ‘Class A’ spectra demonstrate a significantly higher response than the target spectrum at longer periods (>0.5 s). This behaviour implies that the V_{S30} criterion for site classification is not always appropriate in these local geological settings, and may have serious implications especially for the design of taller buildings that respond to lower frequencies of ground shaking.

In the same way, 14 sites were estimated to have a V_{S30} between 360 and 800 m/s, classifying them as EC8 Site Class B. The middle panel of Fig. 5 shows the computed response spectra for these sites and the EC8 target spectrum for Class B. The majority of the spectra lie well over the design spectrum, especially at longer periods. The response spectrum for Majjistral, for example, peaks at $T=0.75$ s, which is outside the horizontal plateau of the design spectrum, and remains considerably higher in the long period part of the spectrum. It can also be noted that for both site classes A and B, at periods shorter than around 0.2 s, the site-specific response spectra fall below the EC8 curves.

One site (Victoria 1, in Gozo) resulted in a V_{S30} value lower than 300 m/s and was thus classified as a Site Class C. In practice, however, the height of the spectrum actually exceeds that of the Class E spectrum (CEN 2004).

The above examples and considerations clearly show the inadequacy of a single criterion such as V_{S30} to characterise all sites, and emphasise the need for site-specific response analysis in cases of a buried clay (or low-velocity) layer geology, especially in the design of important and tall structures.

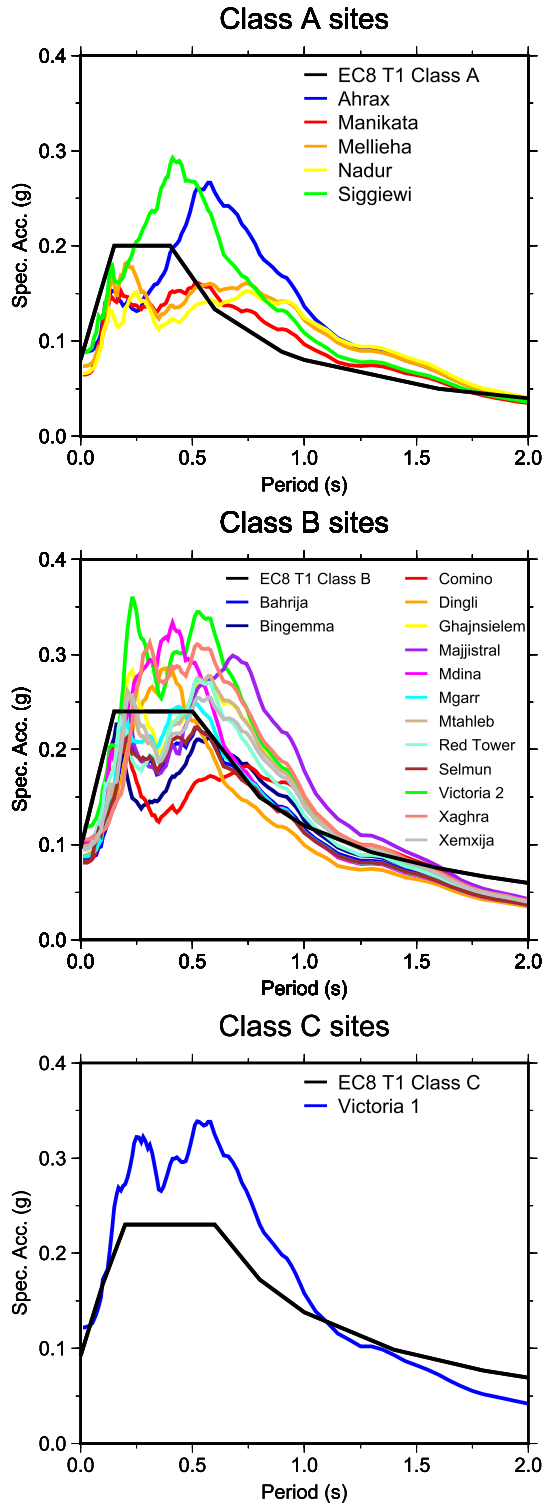
4.2 Amplification factors

A more quantitative comparison of surface ground motion at the investigated sites is provided by computing the following amplification factors from the 5% damped elastic response spectra:

$$F_{\text{PGA}} = \frac{\text{PGA}_{\text{output}}}{\text{PGA}_{\text{input}}}; \quad (1)$$

$$\text{FA} = \frac{\text{SA}_{\text{output}}}{\text{SA}_{\text{input}}}; \quad (2)$$

Fig. 5 The surface response spectra obtained at each site compared to the EC8 recommended site spectra (black line), grouped in class A, B and C sites according to their V_{S30} values



$$FV = \frac{SV_{\text{output}}}{SV_{\text{input}}} \tag{3}$$

where the input values are obtained from the mean spectrum in Fig. 3 whilst the output values are obtained from the mean output spectra shown in Fig. 5. SA and SV are obtained as follows [using the suggestions by Working Group MS (2015)]:

$$SA = \frac{\int_{0.5TA}^{1.5TA} S_a dt}{TA} \tag{4}$$

where TA is the period at which the spectral acceleration (S_a) is maximum (also called the predominant period, refer to top panel in Fig. 6); and

$$SV = \frac{\int_{0.8TV}^{1.2TV} S_v dT}{0.4TV} \tag{5}$$

with TV representing the period at which the velocity response spectrum (S_v) is maximum (refer to Fig. 6, middle panel).

We note that TA is generally smaller than TV and that the integral in SA is generally determined over a range that includes shorter periods. Compagnoni et al (2011) deduce that the two amplification factors may be associated with different dominant periods: FA is more relevant at shorter periods (<0.5 s) whilst FV may be related to the behaviour at longer periods, and thus more relevant in the case of taller buildings. These values provide a convenient way of summing up some of the characteristics of the response spectra. The values of F_{PGA} , FA and FV are mapped in Fig. 7.

The amplification factors may be used to predict ground surface response to an earthquake input. As can be seen in Fig. 7, for the studied sites, values for F_{PGA} and FA are generally both larger than 1, except in a minority of cases. Whilst the latter means that these sites are capable of deamplifying the input ground motion, amplification is expected in the majority of the sites. The three sites for which the F_{PGA} is less than 1 are characterised by a UCL thickness greater than 48 m and are thus classified as class A according to the EC8 site classification. It is worth noting however that even though the Bingemma site is characterised by 52 m of UCL, the PGA is still slightly amplified. This could be due to the fact that the UCL is ‘layered’ into two strata with the upper layer having an average V_s of 600 m/s. In contrast, the highest F_{PGA} values were obtained for those sites where a thin layer of UCL limestone (less than 10 m) outcrops. This is also similar for the amplification factor FA.

On the other hand, the amplification factor FV is greater than 1 at all sites, indicating that amplification is expected at longer periods. Compagnoni et al (2011) also obtained high FV amplification values for sites characterised by a low-velocity layer. In general, for FV, the same relationship was obtained as for FA, i.e. sites with thicker UCL exhibited lower amplification values. However, other characteristics of the V_s profiles also play an important role. For example, a higher FV value was obtained at the Majjistral site, which is characterised by a UCL thickness of 24 m, compared to sites which have a thinner UCL layer (e.g. Mdina which has a UCL thickness of 7 m). This could be interpreted as being due to the high impedance contrast (around 4) between the BC and GL layer at the Majjistral site.

We have investigated possible correlations between the amplification factors and various parameters of the V_s profiles. Figure 8 shows the three amplification factors plotted

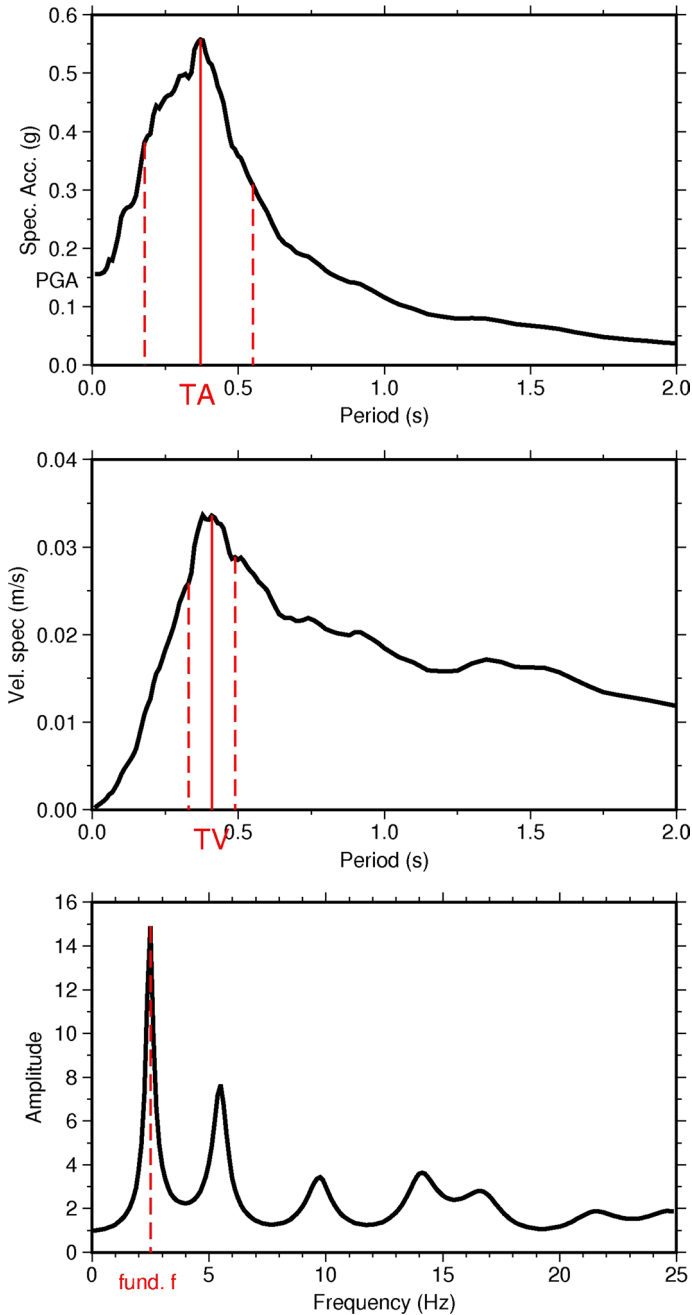


Fig. 6 An example showing the procedure adopted to obtain the amplification factors. Top panel shows how the PGA and TA are determined from the 5% damped acceleration response spectrum. The shaded section shows the integral calculated in Eq. (4). Middle panel shows the identification of TV and the corresponding integral in Eq. (5) from the 5% damped velocity response spectrum. Bottom panel shows how the fundamental frequency is determined from the resulting transfer function

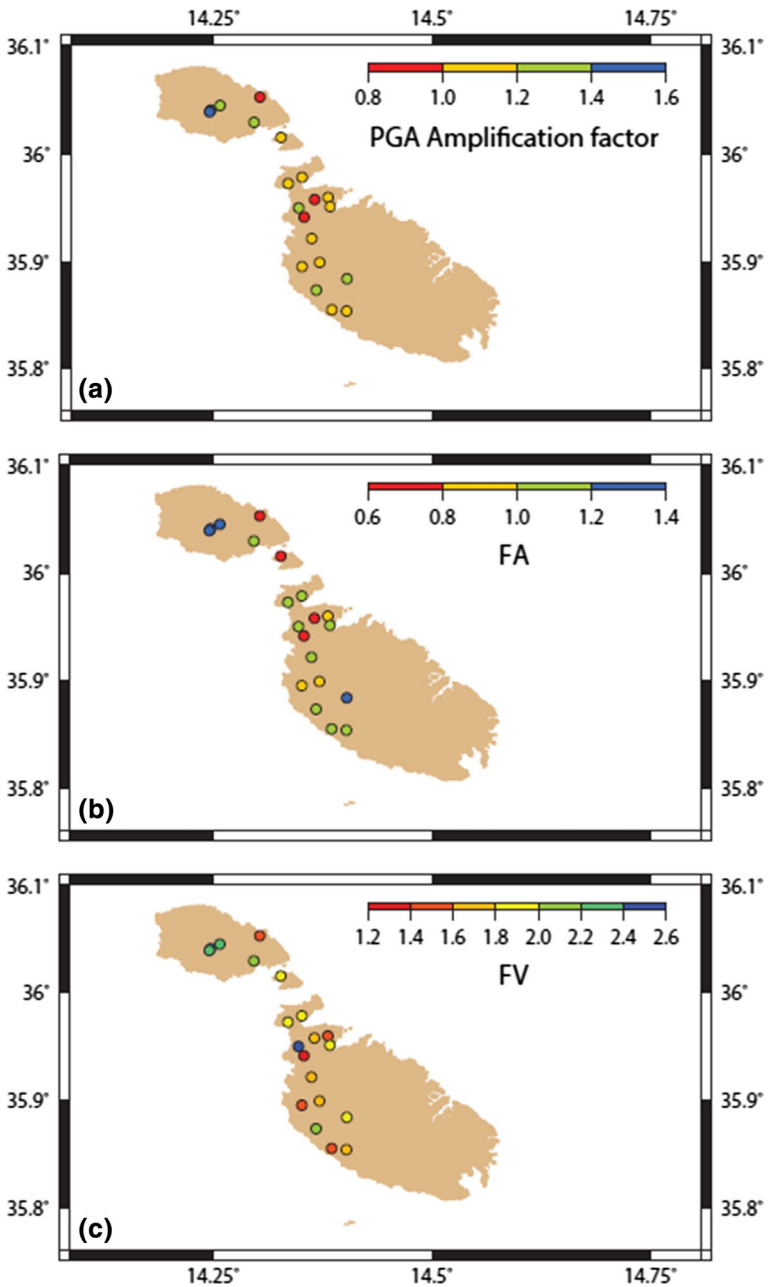


Fig. 7 The amplification factors (F_{PGA} , FA and FV) obtained for each site

against the thickness and V_S of the UCL and BC, the impedance contrast between the BC and underlying GL layer and the V_{S30} . No clear trend is observed for the BC thickness. On the other hand, the FV values increase significantly with decreasing UCL thickness as well as with decreasing UCL and BC shear-wave velocities. These trends are also clear

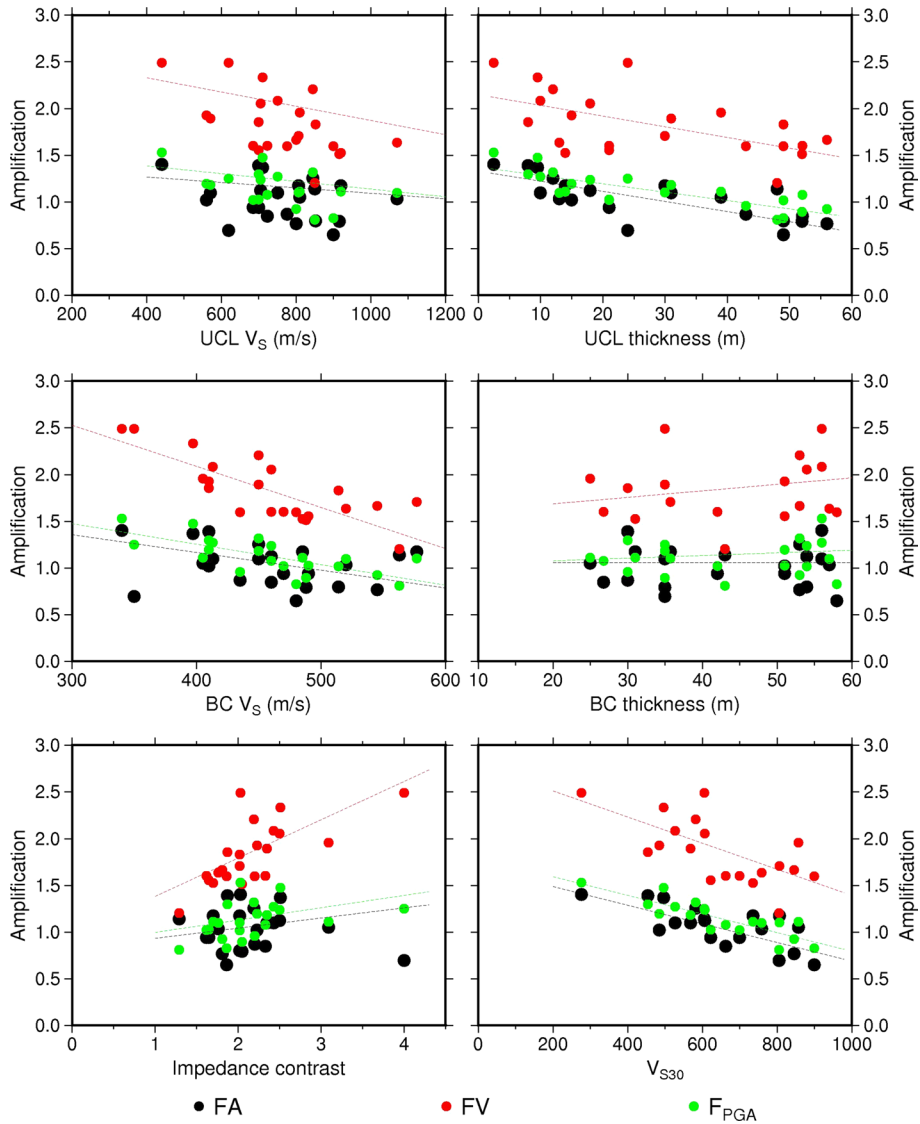


Fig. 8 Graphs showing the variation of the amplification factors with V_S profile characteristics: Top panel for UCL layer characteristics; middle panels for the BC layer; bottom left impedance contrast between BC and GL and bottom right V_{S30}

for F_{PGA} and FA, particularly with respect to BC shear-wave velocity. A clear trend can also be observed between FV and the impedance contrast, whereby the FV increases with impedance contrast. Lastly, the three amplification factors can be seen to decrease with an increase in V_{S30} . However, a large scatter in the FV values can be seen. The observations made above clearly highlight the role that the different properties which constitute the V_S profile play in site amplification and the difficulty in classifying the sites in rigid groups according to the properties of their upper 30 m of subsoil.

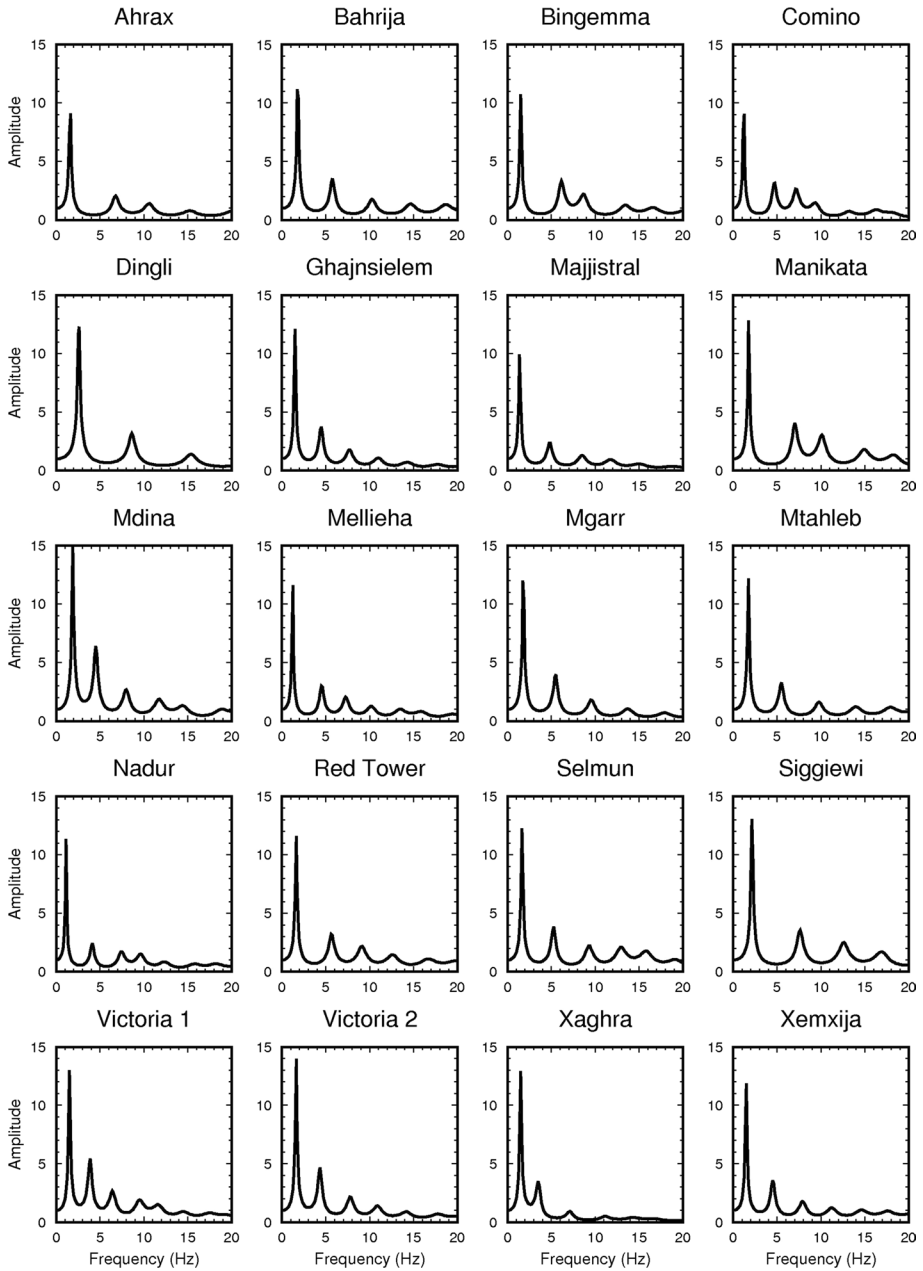


Fig. 9 The transfer functions obtained for each site

The transfer functions obtained for each site are shown in Fig. 9. The fundamental frequency obtained from the 1D transfer function (as shown in Fig. 6, bottom panel) and the predominant period, or TA (as defined above), are tabulated in Table 3, together with the H/V peak frequency obtained at each site as in Farrugia et al. (2016). The fundamental

Table 3 The experimental H/V peak frequency (refer to Farrugia et al. 2016), the calculated fundamental frequency and the predominant period (TA) and predominant frequency (1/TA) obtained for each study site

| Site | H/V peak frequency (Hz) | Fundamental frequency (Hz) | Predominant period (s) | Predominant frequency (Hz) |
|-------------|-------------------------|----------------------------|------------------------|----------------------------|
| Ahrax | 1.5 | 1.63 | 0.58 | 0.58 /1.72 |
| Bahrija | 1.25 | 1.75 | 0.52 | 0.52/1.92 |
| Bingemma | 1.47 | 1.5 | 0.16 | 0.16/6.25 |
| Comino | 0.94 | 1.25 | 0.14 | 0.14/7.14 |
| Dingli | 1.66 | 1.5 | 0.38 | 0.38/2.63 |
| Ghajnsielem | 1.34 | 1.5 | 0.23 | 0.23/4.35 |
| Majjistral | 1.22 | 1.38 | 0.68 | 0.68/1.47 |
| Manikata | 1.38 | 1.75 | 0.52 | 0.52/1.92 |
| Mdina | 1.84 | 1.88 | 0.41 | 0.41/2.44 |
| Mellieha | 1.38 | 1.25 | 0.21 | 0.21/4.76 |
| Mgarr | 1.75 | 1.75 | 0.52 | 0.52/1.92 |
| Mtahleb | 1.34 | 1.75 | 0.57 | 0.57/1.75 |
| Nadur | 1.38 | 1.13 | 0.74 | 0.74/1.35 |
| Red Tower | 1.41 | 1.63 | 0.52 | 0.52/1.92 |
| Selmun | 1.47 | 1.63 | 0.52 | 0.52/1.92 |
| Siggiewi | 1.50 | 2.13 | 0.41 | 0.41/2.44 |
| Victoria 1 | 1.47 | 1.5 | 0.57 | 0.57/1.75 |
| Victoria 2 | 1.41 | 1.63 | 0.23 | 0.23/4.35 |
| Xaghra | 1.31 | 1.5 | 0.31 | 0.31/3.23 |
| Xemxija | 1.31 | 1.5 | 0.23 | 0.23/4.35 |

frequencies obtained are in the range 1–2 Hz except for Siggiewi, for which a value slightly higher than 2 was obtained. These are in agreement with the values obtained using the H/V method. The resulting predominant periods range between 0.15 and 0.75 s. Both the fundamental and predominant periods obtained fall in the range of resonance frequencies of typical 2–10 storey buildings (Galea et al. 2015; Panzera et al. 2016), which are becoming increasingly common in the northern part of the islands where the clay is present. Consequently, these buildings might suffer significant damage when this scenario is considered.

In the following sections, the effect of the UCL layer on the surface response spectra and the validity of parameters such as V_{S30} and $V_{Sbedrock}$ for site response analysis will be investigated.

4.3 The effect of the outcropping Upper Coralline Limestone layer

Whereas a site with outcropping clay is normally perceived as vulnerable within the local construction industry, sites on outcropping UCL may often be regarded as ‘rock sites’ without adequate consideration of the effect of the underlying clay. To assess the extent to which the top UCL layer mitigates the amplification effect of the clay, site response analysis was again carried out on the profiles with the UCL layer being removed, equivalent to a surface geology with outcropping Blue Clay. The other profile properties were kept as in the previous analysis. The resulting response spectra for both cases (referred to as With and

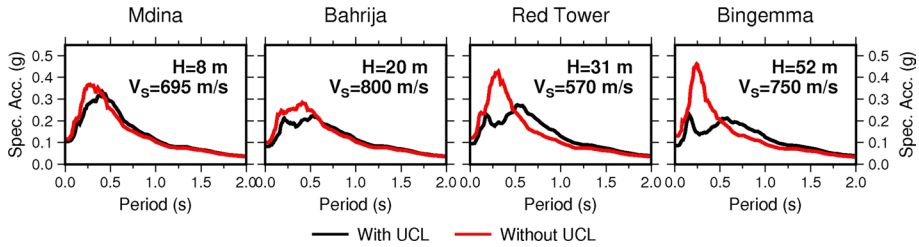


Fig. 10 The resulting surface response spectra for V_S profiles with and without the UCL layer. The V_S and thickness H of the UCL layer which was removed are indicated

Without UCL) are presented in Fig. 10. The thickness, H , and V_S of the UCL layer are also given in the figure for each site.

From the resulting acceleration spectra, it can be noted that the response spectra for sites with a thin UCL layer (up to around 20 m) remain very similar if the UCL layer is removed, i.e. the BC is outcropping. However, as the UCL gets thicker, the amplification effect is considerably reduced, mostly at periods below 1 s. Thus, it can be concluded that the UCL acts as a medium which decreases surface ground motion and absorbs short periods. It, therefore, offers some ‘protection’ especially when having a considerable thickness. Its effect, however, is almost negligible when having a thin UCL layer (less than around 20 m).

4.4 The relevance of V_{S30} , $V_{Sbedrock}$ and site classification of building codes

We argue that V_{S30} is not an adequate proxy to characterise the amplification potential of a site, especially in the type of geological situation being considered here. This has already been recognized by other authors (eg Pitilakis et al. 2013; Gallipoli and Mucciarelli 2009) who have also suggested the use of the travel-time average shear-wave velocity down to the bedrock ($V_{Sbedrock}$) as an alternative.

To further show that both V_{S30} and $V_{Sbedrock}$ may be inadequate, we have randomly constructed a number of different shear-wave velocity profiles (4 of which are shown in Fig. 11), all having the same V_{S30} ($670 \text{ m/s} \pm 15 \text{ m/s}$), $V_{Sbedrock}$ ($625 \text{ m/s} \pm 15 \text{ m/s}$) and characterised by a buried low-velocity layer. The V_{S30} values classify the profiles as EC8 Class B sites. Within the profiles, the shear-wave velocity and thickness of each layer (UCL, BC, GL) were constrained to be within the ranges of values measured in the study, shown in Table 4. The numerical analysis was conducted again for each of these profiles using the same input time histories and curves as in Sects. 3.2 and 3.3. The resulting spectra for four such profiles, together with the Type 1 EC8 spectra, are presented in Fig. 11.

The computed acceleration spectra clearly show significant differences between the response spectra at a wide range of periods. Specifically, the PGA varies from 0.068 g to 0.1 g and the maximum spectral acceleration varies from 0.2 g to almost 0.35 g. Comparing with the EC8 design spectra, it can be observed that whilst profile 2 has a similar spectrum to the EC8 site class B design spectrum, the other profiles are more similar to other site classes. In particular, the spectrum of profile 4 can be compared with the site class A spectrum, profile 3 with site class C, whilst profile 1 can be seen to exceed the response of a class E site. This comparison highlights the inadequacy of the V_{S30} and $V_{Sbedrock}$ proxies

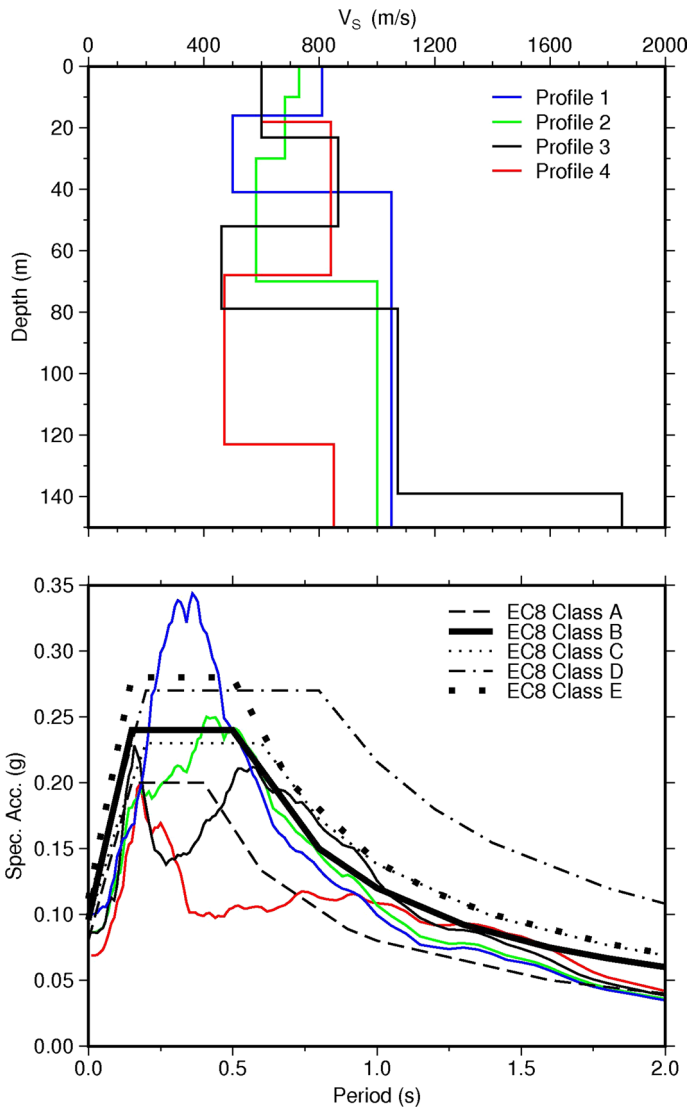


Fig. 11 Top panel: Four hypothetical V_s profiles with similar V_{s30} and $V_{sbedrock}$. Bottom panel: The resulting 5% damped surface response spectra of the profiles from the top panel and the EC8 design spectra. Colours correspond to the top panel

Table 4 Ranges used for the construction of random V_S profiles

| Parameter | Range |
|---------------|--------------|
| UCL thickness | 0–60 m |
| UCL V_S | 500–1100 m/s |
| BC thickness | 0–60 m |
| BC V_S | 350–600 m/s |
| GL thickness | 20–100 m |
| GL V_S | 700–1400 m/s |

and continues to support the idea that site-specific response analysis is required for sites characterised by a buried low-velocity layer.

5 Conclusions

In this study, the local seismic response in regions of the Maltese islands, where a low-velocity clay layer is buried underneath limestone, is evaluated using the equivalent linear numerical code SHAKE2000. The stratigraphic sequence of 20 sites in terms of shear-wave velocities was previously obtained using geophysical investigations. The V_S profiles together with dynamic soil properties and design acceleration time histories were used as inputs to SHAKE2000 to provide the acceleration response spectra at each site. The results were also represented in terms of three amplification factors: F_{PGA} , FA and FV. Significantly, it has been observed that sites with a thin capping of UCL above the clay layer exhibit high amplification factors. However, it was also noted that the other properties of the V_S profiles such as the impedance contrast can contribute to high FV amplification values. The predominant period and fundamental frequencies obtained from the 1D numerical simulation coincide with resonance frequencies of typical 2–10 storey buildings, which are becoming increasingly common in the northern part of the islands where the clay is present.

The comparison between the site-specific 5% damped elastic response spectra and the corresponding recommended EC8 spectra showed that the response spectrum of the majority of the sites significantly exceeds the EC8 spectra at the plateau periods of the design spectrum and at longer periods. Moreover, it was shown that layered structures having different V_S profiles but having the same V_{S30} and $V_{Sbedrock}$ can produce different ground motion response, with an amplification differing by a factor of 2 or more at certain periods. This indicates that these two parameters may not be suitable proxies for site amplification, at least for sites characterised by velocity inversions.

Finally, the role of the UCL layer in the local site response was investigated by re-running the numerical analysis using the same profile but with the UCL layer removed. The comparison between the response spectra of the profiles with and without UCL shows that the spectral acceleration decreases considerably as the upper layer gets thicker.

Our results highlight the inadequacy of using V_{S30} or $V_{Sbedrock}$ to generalise the behaviour of different sites using one design response spectrum, especially in areas where the geology is not a simple case of a low-velocity sedimentary layer over bedrock, but may include different situations such as a thick, buried low-velocity layer. This situation is common both locally and globally. In such cases, it is important that site-specific response investigations are conducted, and that such a practice is included in an updated building

code for the country, together with further microzonation studies, numerical modelling and studies on building behaviour. The site response results obtained in this study show that even if the national seismic hazard is low-to-moderate, the rapidly increasing number of constructions on geologically vulnerable areas imparts a high risk, even at moderate levels of ground shaking. A holistic risk assessment of the islands, which takes all the above into consideration, is therefore of crucial importance.

Acknowledgements This work was supported by the Endeavour Scholarship scheme financed out of Government of Malta national fund. Some figures were created using the Generic Mapping Tools (Wessel and Smith 1998)

Funding This work was supported by the Endeavour Scholarship scheme financed out of Government of Malta national fund.

Code availability SHAKE2000 and GMT-available.

Compliance with ethical standards

Conflict of interest The authors declare that they have no conflict of interest.

References

- Barani S, De Ferrari R, Ferretti G (2013) Influence of soil modelling uncertainties on site response. *Earthq Spectra* 29:705–732
- Bommer JJ, Acevedo AB (2004) The use of real earthquake accelerograms as input to dynamic analysis. *J Earthq Eng* 8:43–91
- Castellaro S, Mulargia F, Rossi PL (2008) Vs30: proxy for seismic amplification? *Seismol Res Lett* 79(4):540–543
- CEN (2004) Eurocode 8: Design of structures for Earthquake Resistance. European Standard. European Committee for Standardisation, Brussels
- Compagnoni M, Pergalani F, Boncio P (2011) Microzonation study in the Paganica-San Gregorio area affected by the April 6, 2009 L'Aquila earthquake (central Italy) and implications for the reconstruction. *Bull Earthq Eng* 9:181–198
- Di Alessandro C, Bonilla LB, Boore DM, Rovelli A, Scotti O (2012) Predominant-period site classification for response spectra prediction equations in Italy. *Bull Seismol Soc Am* 102:680–695
- Di Giacomo D, Gallipoli MR, Mucciarelli M, Parolai S, Richwalski SM (2005) Analysis and modeling of HVSR in the presence of a velocity inversion: the case of Venosa, Italy. *Bull Seismol Soc Am* 95:2364–2372
- Farrugia F, Paolucci E, D'Amico S, Galea P (2016) Inversion of surface-wave data for subsurface shear-wave velocity profiles characterised by a thick buried low-velocity layer. *Geophys J Int* 206:1221–1231
- Frankel A, Carver D, Williams R (2002) Nonlinear and linear site response and basin effects in Seattle for the M6.8 Niqually, Washington, earthquake. *Bull Seismol Soc Am* 92:2090–2109
- Galea P (2007) Seismic history of the Maltese islands and considerations on seismic risk. *Ann Geophys* 50:725–740
- Galea P, Micallef T, Muscat R, D'Amico S (2015) Resonance frequency characteristics of buildings in Malta and Gozo using ambient vibrations. In: *Georisks in the mediterranean and their mitigation*, Mistal Press, p 262
- Gallipoli MR, Mucciarelli M (2009) Comparison of site classification from VS30, VS10, and HVSR in Italy. *Bull Seismol Soc Am* 99:340–351
- Gatt P, Tucker M, Davies R, Pascucci V, Andreucci S (2009) Drowning of the Malta carbonate platform: facies and sequence stratigraphy of the Lower Coralline Limestone (U. Oligocene). In: *Abstract Book, 27th IAS Meeting of Sedimentology, Alghero, 20–23 September* (p 18). 27th IAS Meeting of Sedimentology
- Gatt P (2012) Carbonate facies, depositional sequences and tectonostratigraphy of the Palaeogene Malta Platform. Ph. D dissertation, Durham University

- Guidoboni E, Ferrari G, Mariotti D, Comastri A, Tarabusi G, Sgatonni G, Valensise G (2018) CFTI5Med, Catalogo dei Forti Terremoti in Italia (461 aC-1997) e nell'area Mediterranea (760 aC-1500)
- Iervolino I, Galasso C, Cosenza E (2010) REXEL: computer aided record selection for code-based seismic structural analysis. *Bull Earthq Eng* 8:339–362
- Luzi L, Puglia R, Pacor F, Gallipoli MR, Bindi D, Mucciarelli M (2011) Proposal for a soil classification based on parameters alternative or complementary to V_{S30} . *Bull Earthq Eng* 9:1877–1898
- Luzi L, Puglia R, Russo E, ORFEUS WG5 (2016) Engineering Strong Motion Database, version 1.0. Istituto Nazionale di Geofisica e Vulcanologia, Observatories & Research Facilities for European Seismology. <https://doi.org/10.13127/ESM>
- Magri O (2006) A geological and geomorphological review of the Maltese islands with special reference to the coastal zone. *Territoris* 6:7–26
- Nakamura Y (1989) A method for dynamic characteristics estimations of subsurface using microtremors on the ground surface. *Q Rep Railw Tech Res Inst Nguyen* 30:25–33
- Ohori M, Nobata A, Wakamatsu K (2002) A comparison of ESAC and FK methods of estimating phase velocity using arbitrarily shaped microtremor arrays. *Bull Seismol Soc Am* 92:2323–2332
- Oil Exploration Directorate (1993) Geological map of the Maltese islands. Office of the Prime Minister, Valletta
- Ordonez GA (2011) User's manual for SHAKE 2000: a computer program for the 1-D analysis of geotechnical earthquake engineering problems. GeoMotions, Washington, DC
- Ozcep T, Ozcep F, Ozel O (2013) V_{S30} , site amplifications and some comparisons: the Adapazari (Turkey) case. *Phys Chem Earth* 63:92–101
- Pace S, Panzera F, D'Amico S, Galea P, Lombardo G (2011) Modelling of ambient noise HVSR in a complex geological area- Case study of the Xemxija Bay Area, Malta. In: Slejko D, Rebez A (eds) Riassunti Estesi Delle Comunicazioni, 30° Convegno Nazionale GNGTS. Trieste, Italy, pp 299–302
- Pagliaroli A, Lanzo G (2008) Selection of real accelerograms for the seismic response analysis of the historical town of Nicastro (Southern Italy) during the March 1638 Calabria earthquake. *Eng Struct* 30:2211–2222
- Panzera F, D'Amico S, Galea P, Lombardo G, Gallipoli MR, Pace S (2013) Geophysical measurements for site response investigation: preliminary results on the island of Malta. *Bollettino di Geofisica Teorica ed Applicata* 54:111–128
- Panzera F, D'Amico S, Lombardo G, Galea P, Akinci A (2015) Overview of the seismic hazard in the Sicily channel archipelagos. In: Lombardo G, Panzera F (eds), Establishment of an integrated Italy-Malta cross border system of civil protection: geophysical aspects, Aracne Editrice, pp 31–45. <https://doi.org/10.4399/97888548825604>
- Panzera F, D'Amico S, Lombardo G, Longo E (2016) Evaluation of building fundamental periods and effects of local geology on ground motion parameters in the Siracusa area. *Italy J Seismol* 20(3):1001–1019
- Park D, Hashash YMA (2004) Probabilistic seismic hazard analysis with nonlinear site effects in the Mississippi Embayment. In: 13th World Conference on Earthquake Engineering
- Pedley HM, House MR, Waugh B (1978) The geology of the Pelagian block: the Maltese Islands. In: The Ocean basins and margins (pp 417–433). Springer, Boston, MA
- Pedley M, Clarke M, Galea P (2002) Limestone Isles in a Crystal Sea: the geology of the Maltese islands. Publishers Enterprises Group Ltd, San Gwann
- Peruzza L, Azzaro R, Gee R, D'Amico S, Langer H, Lombardo G, Pace B, Pagani M, Panzera F, Ordaz M, Suarez ML, Tusa G (2017) When probabilistic seismic hazard climbs volcanoes: the Mt. Etna case, Italy-Part 2: computational implementation and first results. *Nat Hazards Earth Syst Sci* 17:1999–2015
- Picozzi M, Albarello D (2007) Combining genetic and linearized algorithms for a two-step joint inversion of Rayleigh wave dispersion and H/V spectral ratio curves. *Geophys J Int* 169:189–200
- Pitilakis K, Riga E, Anastasiadis A (2013) New code site classification, amplification factors and normalized response spectra based on a worldwide ground motion database. *Bull Earthq Eng* 11:925–966
- Smerzini C, Galasso C, Iervolino I, Paolucci R (2014) ground motion record selection based on broadband spectral compatibility. *Earthq Spectra* 30:1427–1448
- Steidl J (2000) Site response in southern California for probabilistic seismic hazard analyses. *Bull Seismol Soc Am* 90:S149–S169
- Stewart JP, Liu A, Choi Y (2003) Amplification factors for spectral acceleration in tectonically active regions. *Bull Seismol Soc Am* 93:332–352
- Vella A, Galea P, D'Amico S (2013) Site frequency response characterisation of the Maltese islands based on ambient noise H/V ratios. *Eng Geol* 163:89–100
- Wald L, Mori J (2000) Evaluation of methods for estimating linear site-response amplifications in the Los Angeles region. *Bull Seismol Soc Am* 90:S32–S42

- Wessel P, Smith WH (1998) New, improved version of generic mapping tools released. *Eos Trans Am Geophys Union* 79(47):579
- Working Group MS (2015). Guidelines for seismic Microzonation. https://www.protezionecivile.gov.it/httpdocs/cms/attach_extra/GuidelinesForSeismicMicrozonation.pdf?
- Yamanaka H, Ishida H (1996) Application of genetic algorithms to an inversion of surface-wave dispersion data. *Bull Seismol Soc Am* 86:436–444
- Zammit-Maempel G (1977) An outline of Maltese geology. Progress Press, Malta

Publisher's Note Springer Nature remains neutral with regard to jurisdictional claims in published maps and institutional affiliations.